The Journal of Chemical Physics ARTICLE scitation.org/journal/jcp

Model of charge transfer collisions between C_{60} and slow ions

Cite as: J. Chem. Phys. 157, 054303 (2022); doi: 10.1063/5.0100357
Submitted: 23 May 2022 • Accepted: 10 July 2022 •
Published Online: 5 August 2022

View Online Export Citation CrossMark

J. Smucker,[1,a)] J. A. Montgomery, Jr.,[1] M. Bredice,[1] M. G. Rozman,[1] R. Côté,[2] H. R. Sadeghpour,[3] D. Vrinceanu,[4] and V. Kharchenko[1,3]

AFFILIATIONS

[1] Department of Physics, University of Connecticut, Storrs, Connecticut 06269, USA
[2] Department of Physics, University of Massachusetts Boston, Boston, Massachusetts 02125, USA
[3] ITAMP, Center for Astrophysics | Harvard & Smithsonian, Cambridge, Massachusetts 02138, USA
[4] Department of Physics, Texas Southern University, Houston, Texas 7704, USA

[a)] **Author to whom correspondence should be addressed:** jonathan.smucker@uconn.edu

ABSTRACT

A semiclassical model describing the charge transfer collisions of C_{60} fullerene with different slow ions has been developed to analyze available observations. These data reveal multiple Breit–Wigner-like peaks in the cross sections, with subsequent peaks of reactive cross sections decreasing in magnitude. Calculations of charge transfer probabilities, quasi-resonant cross sections, and cross sections for reactive collisions have been performed using semiempirical interaction potentials between fullerenes and ion projectiles. All computations have been carried out with realistic wave functions for C_{60}'s valence electrons derived from the simplified jellium model. The quality of these electron wave functions has been successfully verified by comparing theoretical calculations and experimental data on the small angle cross sections of resonant $C_{60} + C_{60}^{+}$ collisions. Using the semiempirical potentials to describe resonant scattering phenomena in C_{60} collisions with ions and Landau–Zener charge transfer theory, we calculated theoretical cross sections for various C_{60} charge transfer and fragmentation reactions which agree with experiments.

Published under an exclusive license by AIP Publishing. https://doi.org/10.1063/5.0100357

I. INTRODUCTION

Charge transfer in ion–atom collisions has been studied intensively for decades, mostly due to high demands in plasma physics, astrophysics, and atmospheric science.[1–3] A detailed understanding of electron transfer processes in ion–atom collisions is at hand, thanks to observations and theoretical analysis involving both quantum and classical mechanics. The most accurate results have been obtained for resonant and quasi-resonant charge transfer because only a few states are involved in the electron capture process. The majority of ion–atom systems do not support resonances between electronic states and are mostly treated in expensive numerical calculations operating with extended basis functions.[4] Recent examples of such multistate calculations can be found in the theoretical analysis of charge transfer collisions of highly charged ions.[5]

Significant simplification can be carried out for the theoretical description of slow collisions, when velocities of heavy nuclei are much smaller than typical electron velocities. In the semiclassical approximation, the motion of heavy particles is considered classically and electronic degrees of freedom are treated quantum mechanically.[6–9] In this model, transitions between different electronic states occur in specific regions of nonadiabatic behavior, such as areas of pseudo-crossing[10–12] or crossing (nonadiabatic transition induced by rotational interactions[7]) of electronic energy curves.

The current development of experimental and theoretical investigations includes investigations of charge transfer collisions with more complex targets, such as molecules, nano-sized clusters, and condensed matter materials.[13–16] These processes are of interest due to their applications in biomedical fields and nanoscience. In these investigations, fullerenes have been especially well studied, as they are an example of nanoparticles with well-defined structure and well-defined electronic properties.[17–20]

In 1992 and 1993, Christian *et al.*[21–25] published a series of papers reporting relative cross sections for various fragmentation and charge transfer reactions involving C_{60}. These papers reported

Published under an exclusive license by AIP Publishing

the relative values of charge transfer cross sections for collisions between carbon, nitrogen, neon, oxygen, lithium, or sodium cations with C_{60}. These relative cross sections were measured as a function of collision energy for pure charge transfer as follows:

$$X^+ + C_{60} \rightarrow X + C_{60}^+, \tag{1}$$

where X is C, O, N, Ne, Na, or Li. They also reported data on the energy dependence of relative cross sections for charge transfer and fragmentation collisions with C_{60},

$$X^+ + C_{60} \rightarrow X + C_{60-2n}^+ + nC_2, \tag{2}$$

where n is an integer. The cross section of C_{59} formation was measured by Christian *et al.* to be significantly smaller than the cross sections for the fragmentation of an even number of carbon atoms (except in the case of the carbon cation). The authors suggested that the ions X^+ and C_{60} fullerene form an intermediate long-lived complex that decays into different reactive channels of fragmentation. For this scenario, each of the reactions shown in Eq. (2) forms a Breit–Wigner-like resonance.

To our knowledge, there has been no detailed theoretical exploration of these reactions for slow ion collisions. This is likely due to the difficulty surrounding theoretical approaches to dynamical properties of the $C_{60} + X^+$ system at different interparticle distances. Even an accurate *ab initio* evaluation of the binding energy of C_2 in C_{60} has already proven to be a difficult computational task.[26,27] In light of this, we have developed a semiempirical model in order to offer theoretical insight into these charge transfer and fragmentation reactions while avoiding expensive *ab initio* calculations. Our model is essentially based on the semiclassical description of the $C_{60} + X^+$ system and on the models of nonadiabatic transitions developed in the theory of atomic collisions.[6–8]

We propose a simplified model, which starts by using the jellium model suggested by Baltenkov *et al.*[28] to describe the electron wave functions in C_{60}. This model is combined with electrostatics and various measured physical parameters of C_{60} to create pseudopotential curves for a positive ion interacting with C_{60}. By using results of the resonant scattering theory of a multichannel collision process and Landau–Zener theory of nonadiabatic transitions between different electronic states,[10–12] we developed a theoretical model that fits the original experimental data obtained for different projectile ions.

II. SIMPLIFIED MODEL OF C_{60} ELECTRONIC STATE

Taking advantage of the symmetry of C_{60}, we use the jellium model suggested by Baltenkov *et al.*[28] We consider charge transfer processes that involve only fullerene valence electrons.

Since C_{60} is a sphere-like object, we can approximate it as producing a potential well that is only a function of the radius r. At large distances, $r \gg R_{C_{60}}$ ($R_{C_{60}}$ being the radius of the C_{60} shell), the leading term of the real electron potential is the Coulomb potential. Therefore, one could write the potential as follows:

$$U(r) = U^*(r) + U_{lr}(r) = U^*(r) - \frac{f(r,a)}{r}, \tag{3}$$

where r is the distance of a valence electron from the center of C_{60}, $U^*(r)$ is the short-range potential, $U_{lr}(r)$ is the long-range potential, and $f(r,a)$ is the Tang–Toennies damping function.[29,30] The Tang–Toennies damping function prevents the long-range Coulomb term from dominating at short ranges; it is given as

$$f(r,a) = 1 - e^{-ar}\sum_{k=0}^{4}\frac{(ar)^k}{k!}, \tag{4}$$

where a is an adjustable parameter that dictates the range at which the function is suppressed. For the short-range part, Baltenkov *et al.* asserts that a Lorentzian potential is more realistic than the proposed alternatives (such as a delta function). This potential is given as

$$U^*(r) = -U_L\frac{d^2}{(r - R_{C_{60}})^2 + d^2}, \tag{5}$$

where U_L is the maximum well depth and the width of the well is given by $2d$. $R_{C_{60}} = 6.665\ a_0$[31] corresponds to the radius of the C_{60} carbon shell. We consider only s-electrons with zero angular momentum. The C_{60} wave function will be affected by the incoming ion and this effect can be different depending on the ion. To account for this, the width of the positive background d was used as a fit parameter for the density of states model, as discussed later in the article. The model pseudo-potential from Eq. (5) provides adequate description of a single electron wave function in the region localized around the C_{60} carbon shell, if an accurate value of the electron energy ε is used as a parameter of the Schrödinger equation. These wave functions will be used to calculate potentials for $C_{60} + X^+$, the long-range behavior of these potential will be calculated using a more accurate method that does not use these wave functions (see Sec. IV). Therefore, we are most concerned with the behavior of the wave function around the C_{60} shell and so we only use the potential shown in Eq. (5) when calculating the wave functions. We solved the Schrödinger equation numerically and obtained the electron wave function for an ε value equal to the experimental value of the photoionization energy for C_{60}, which is about 7.58 eVs according to De Vries *et al.*[32]

We solved the Schrödinger equation using a Verlet algorithm and adjusted the well depth U_L until the wave function converges to zero as r approaches infinity, indicating that 7.58 eVs had become an eigenvalue. We found that $d = 0.5a_0$, $d = 0.32a_0$, and $d = 0.28a_0$ obtained good results for the oxygen ion, nitrogen ion, and neon ion cross sections, respectively (this will be discussed later). Since the energy is held constant, adjusting d has a minimal effect on the wave functions. For $d = 0.5a_0$, $d = 0.32a_0$, and $d = 0.28a_0$, we found $U_L = 0.88a_0$, $U_L = 1.19a_0$, and $U_L = 1.31a_0$[33] respectively. The resulting wave functions are shown in Fig. 1.

III. TEST OF THE ELECTRON WAVE FUNCTIONS: RESONANT CHARGE TRANSFER

We calculate the total cross sections for the resonant charge transfer case to test the accuracy of the one-electron wave functions obtained with the jellium model. The reaction for this case is $C_{60}^+ + C_{60} \rightarrow C_{60} + C_{60}^+$. We use the Holstein–Herring method[34] as it simplifies the cross section so it only depends on the single particle electronic wave function. This method is briefly discussed below. A schematic of this method is shown in Fig. 2.

Published under an exclusive license by AIP Publishing

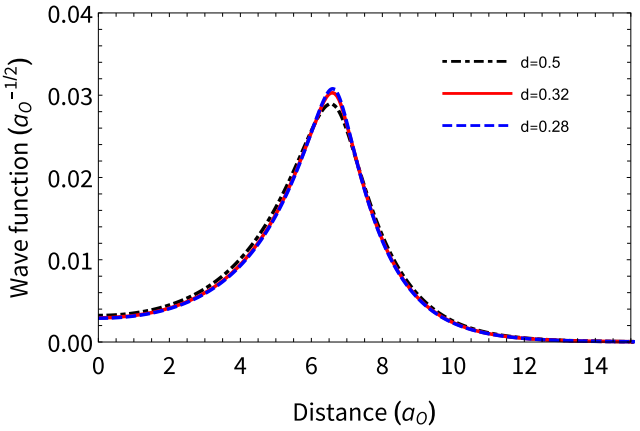

FIG. 1. The electron wave functions calculated for C_{60} using the jellium model. The black dotted and dashed curve corresponds to $d = 0.5a_0$ and $U_L = 0.88a_0$. The blue dashed curve corresponds to $d = 0.28a_0$ and $U_L = 1.19a_0$. The red solid curve corresponds to $d = 0.32a_0$ and $U_L = 1.31a_0$. The value of d was chosen so the results of the density of states model (see Sec. V A) matched the data.[21–23]

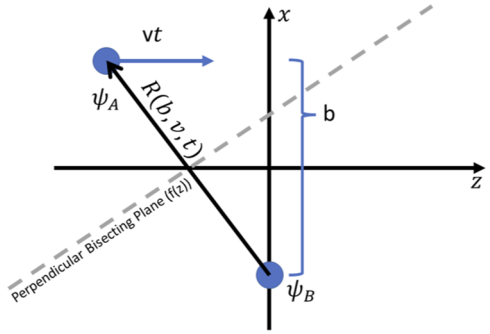

FIG. 2. chematic of the method used to calculate the small angle charge transfer cross section for $C_{60} - C_{60}^+$. The unperturbed valence electron wave functions for the two C_{60} molecules are represented by ψ_A and ψ_B. ψ_A and ψ_B are the same wave functions except for a spatial shift. ψ_A moves at a constant speed v in the z-direction. The gray dashed line represents the plane halfway between the two C_{60} molecules. This plane rotates as time passes.

The electrons of the $C_{60} - C_{60}^+$ pair move much faster than the colliding molecule. Therefore, the electron energies and wave functions adjust promptly to any change of the inter-fullerene distance $R(b, v, t)$ (where b is the impact parameter, v is the velocity, and t is time). For the considered interval of collision energies, the fullerene motion is classical; more specifically, it is a straight line trajectory, if $R(b, v, t)$ is larger than the diameter of the C_{60} carbon shell. The charge transfer cross section is calculated using the following:

$$\sigma = \int_0^\infty 2\pi b\, P(b, v)\, db, \tag{6}$$

where $P(b, v)$ is the probability of charge transfer occurring. Assuming a system of two $C_{60} - C_{60}^+$ states, which are degenerated as $R(b, v, t) \to \infty$, the $C_{60} - C_{60}^+$ valence electron wave function can be approximated as the gerade and ungerade sums of two C_{60} valence electron wave functions $\psi(\mathbf{r})$. If we also assume an adiabatic process, the probability of the resonant charge transfer collisions $P(v, b)$ can be calculated using the energy splitting between the gerade and ungerade quasi-molecular states as

$$P(v, b) = \sin^2 \int_{-\infty}^{\infty} \frac{\varepsilon_g - \varepsilon_u}{2} dt, \tag{7}$$

in atomic units. This energy splitting can be estimated using the electron probability flux through the plane halfway between the two C_{60} molecules, i.e.,

$$\varepsilon_g - \varepsilon_u = 2 \int_{-\infty}^{\infty} \int_{-\infty}^{\infty} \psi(f(z) + b/2, y, z) \nabla \psi(f(z) + b/2, y, z) \cdot \frac{\vec{R}(b, v, t)}{\|\vec{R}(b, v, t)\|} dy\, dz, \tag{8}$$

where $\psi(\mathbf{r})$ is the valence electron wave function of an unperturbed C_{60} molecule. The above equation is again in atomic units. For lowest order perturbation theory, we can use the jellium wave functions. More accurate theoretical models take into account a wave function transformation induced, at large distances, by the ion. We have chosen the impact parameter b to be along the x axis and the two particles to be shifted by $\pm b/2$ from the origin. The moving projectile was chosen to move along the z axis at a constant speed v starting at $z = -\infty$. The $f(z)$-function characterizes the plane that is the perpendicular bisector for the two C_{60} molecules (the gray dashed line in Fig. 2). In this case, $f(z)$ is given as

$$f(z) = -\frac{vt}{b} z + \frac{v^2 t^2}{2b}. \tag{9}$$

This plane rotates with time, and at $t = 0$, it is equivalent to the y-z plane. We would like to study only elastic collisions with charge transfer so the impact parameter has a minimum of $2R_{C_{60}}$. If $b < 2R_{C_{60}}$, then the two C_{60} carbon shells would collide, resulting in other collision processes and non-straight line trajectories. The resulting calculated cross section compared to data reported by Rohmund and Campbell for small angle scattering[35] is shown in Fig. 3. We repeated this calculation using two different values for the parameter d. The changing of d made a small difference in the cross section; this indicates that the parameter d can be adjusted. The calculations are in good agreement with the measured small angle cross sections, indicating that the jellium model wave functions are adequate. It is important to note that Glotov and Campbell later corrected the total cross sections reported by Rohmund and Campbell[35] by taking into account large scattering angles.[36] The theory we used assumes straight line trajectories so the original data on the small angle charge transfer cross section are more applicable. The presence of large angle scattering in resonant charge transfer collisions has not been observed (to our knowledge) in ion–atom collisions or in collisions involving simple molecules. A new theoretical model should be developed to describe resonant charge transfer collisions with large scattering angles.

Published under an exclusive license by AIP Publishing

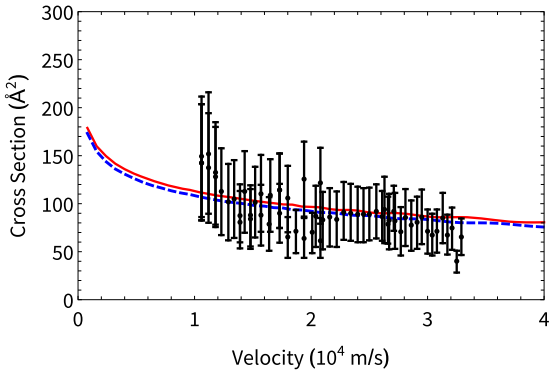

FIG. 3. The small angle cross section for $C_{60} + C_{60}^+$ resonant charge transfer. The black dots represent data from Rohmund and Campbell.[35] The curves are theoretical calculations made using the wave functions from the jellium model, shown in Fig. 1. The red line corresponds to $d = 0.5a_0$ and the blue dashed line corresponds to $d = 0.28a_0$. The adjustment of the parameter d has little effect on the small angle cross section.

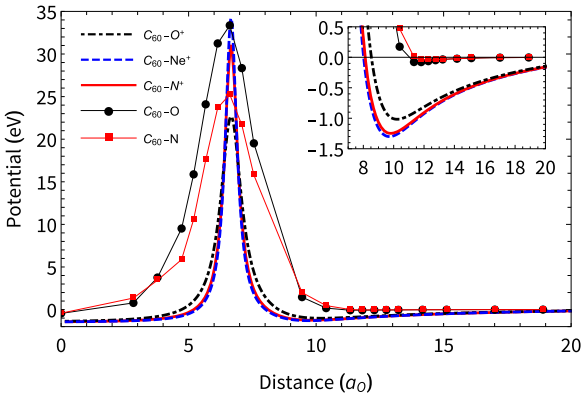

FIG. 4. The potential constructed for C_{60} interacting with a positive ion. The curves are our model potentials and the points represent DFT calculations. The wave function used for the oxygen, nitrogen, and neon potentials are shown in Fig. 1. The long-range behavior of the potentials are shown in the inset.

IV. PSEUDO-POTENTIALS

A simplified description of collision processes involving complex systems can be achieved with the introduction of pseudo-potentials.[37,38] A large number of quasi-molecular states are involved in the considered charge transfer and fragmentation processes. We have constructed pseudo-potentials that describe resonant scattering and charge transfer processes as an evolution of $C_{60} + X^+$ quasi-molecular states. The long-range asymptotic behavior of our potentials corresponds to the long-range interactions in $C_{60} + X^+$ and $C_{60}^+ + X$ systems. Modeling molecular interactions using electrostatic potentials is a well-known technique, which is especially effective for long-range interactions. We combine this technique with the wave functions calculated using the jellium model to calculate the potential energies for C_{60} interacting with a positive ion. To this end, we convert the wave functions shown in Fig. 1 to charge distributions, these charge distributions distribute one negative charge (due to the valence electron). The potential from this one negative charge is added to the potential of the jellium positive background [i.e., Eq. (5)]. For the long-range behavior, C_{60} is treated as a dielectric sphere. The charged ion induces an image point and a line charge inside C_{60}.[39] This image is responsible for a weak attractive force outside the spherical shell. The dielectric constant was set to $\varepsilon_r = 4$ based on results by Ren *et al.*[40] and Ortiz-López *et al.*[41] At large distances, this attractive polarization roughly behaves as a r^{-4} potential. To prevent the long-range potential from dominating at shorter ranges, the long-range potential is multiplied by a Tang–Toennies damping function,[29] which is shown in Eq. (4). In this case, a is chosen so the long-range potential has as little effect on the short-range potential as possible while keeping the long range well as deep as possible. The potential created by the dielectric approximation is much stronger than the typical approach approximating the long range well as being a result of the polarizabilities of the two molecules. The resulting potential is depicted in Fig. 4 with the long-range behavior shown in the inset.

For comparison with the pseudo-potentials, density functional theory (DFT) calculations were performed using the recently developed APFD dispersion corrected hybrid functional[42] and the 6 − 31 + G(d) Gaussian basis set. This method was designed to provide an accurate description of long-range molecular interactions. A comparison of the pseudo-potentials and DFT potentials for C_{60} interacting with oxygen and nitrogen is shown in Fig. 4. $C_{60} + O^+$ is not the ground state of the system; therefore, it is difficult to perform a DFT calculation of this configuration, which is why we performed the potential energy curve calculation for $C_{60} + O$. Both the DFT calculations and the pseudo-potentials predict a high peak at $6.665a_0$ and two shallow wells: one within the C_{60} shell and one directly outside the C_{60} shell. All DFT calculations were performed with the Gaussian 16 electronic structure programs.[43]

Although not directly included in the calculation of the C_{60}–ion interaction, the electron wave function is slightly disturbed by the presence of the ion. Such influence can be accurately determined at large distances r between the projectile ion and C_{60}, but it requires elaborate numerical computation. The most simple empirical way to take into account the charge's interaction with the electronic states of C_{60} is to include a dependence of the width parameter d in Eq. (5) on the projectile.

Quasi-molecular charge transfer theory also requires potentials for C_{60}^+ interacting with a neutral atom in both ground and excited states in order to locate regions where adiabatic charge transfer can occur. At large distances between the C_{60}^+ molecule and the atom, the charge around the C_{60}^+ molecule induces a dipole in the neutral atom. The magnitude of this dipole is dependent on the polarizability of the neutral atom. The long-range potential $V(r)$ of the interaction between C_{60}^+ and the neutral atom with polarizability α_X behaves as $V(r) = -\alpha_X/2r^4$. A set of potentials for the $C_{60}^+ + X$ interaction (with X representing O, N, and Ne) has been computed. These potentials are shown in Fig. 5. The polarizabilities α used are $\alpha = 0.802$ Å^3 for oxygen,[44,45] $\alpha = 1.10$ Å^3 for nitrogen,[44,45] and $\alpha = 0.382$ Å^3 for neon.[46] The polarizabilities vary depending on the state but do not vary significantly; so, for simplicity,

Published under an exclusive license by AIP Publishing

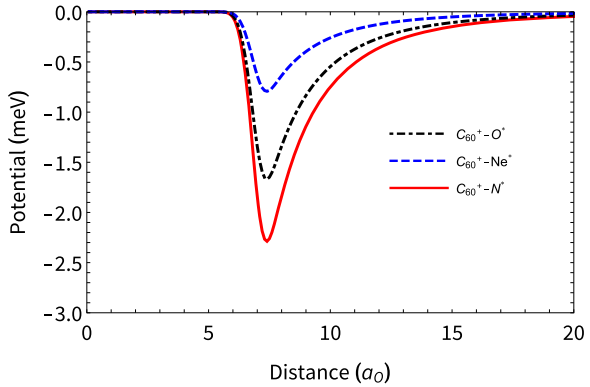

FIG. 5. The potentials constructed for C_{60}^+ interacting with oxygen (black dashed and dotted line), nitrogen (red line), and neon (blue dashed line). The potential was calculated using the polarizabilities of the atoms interacting with a positively charged spherical shell. To avoid non-differentiable points, the potentials where made smooth by applying a Gaussian filter. This potential should be accurate for longer ranges.

we only used the ground state polarizabilities. These potentials are likely not accurate inside or near the spherical shell but should be more accurate on longer ranges since the polarization potential is the dominating term for large distances. Since the relevant regions of nonadiabatic interaction (which are needed for Landau–Zener charge transfer theory) between the two potentials are located at long ranges, these potentials should be accurate enough in the region of interest.

V. NON-RESONANT CHARGE TRANSFER AND FRAGMENTATION

Christian *et al.*[21–23] proposed that the fragmentation occurs separately from charge transfer. They proposed that when charge transfer occurs, the resulting C_{60}^+ is in a rovibrational state that allows the process to be near resonant. Since C_{60} has many rovibrational states, there is likely a state that allows for this. This rovibrational state is proposed to be unstable and the C_{60}^+ then decays into $C_{60-2n}^+ + nC_2$. We used the potentials constructed in Sec. IV to create a reaction pathway model that can explain uniquely the experimental set of data on the charge transfer collisions between slow ions and C_{60}.[21–24] We treat the charge transfer and the fragmentation of C_{60} separately (as Christian *et al.* proposed), multiplying the results from both together to obtain the final results. The fragmentation is treated as an inelastic scattering process using a density of states model. Charge transfer is modeled using Landau–Zener charge transfer theory. A schematic representation of our model is shown in Fig. 6. The curves in Fig. 6 represent effective potentials of different reactive channels. According to Landau–Zener theory, it is near the intersection between these channels that the state may change.

A. Density of states

We estimate parameters of the states involved in the resonant scattering process. The potential shown in Fig. 4 is part of the effective potential of radial motion. The full potential of the collision contains the centrifugal potential which depends on the impact parameter b. This term affects the depth and shape of the interior potential well. For large b, the total potential becomes completely dominated by the centrifugal term; this occurs somewhere around $b \approx 8a_0$ depending on the projectile and its kinetic energy.

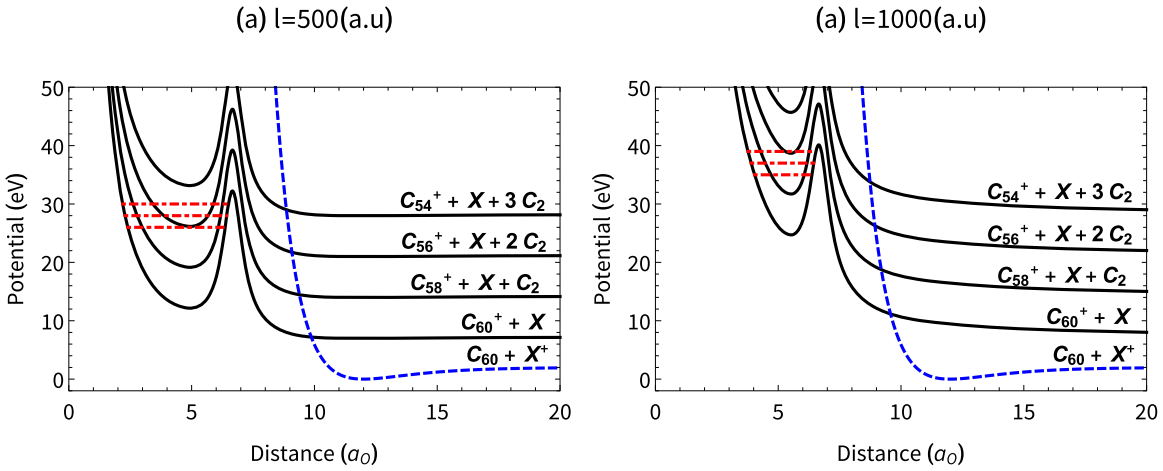

FIG. 6. Above are two sketches representing our model. The black lines represent potentials for $C_{60-2n}^+ + X + nC_2$, where n is 0, 1, 2, or 3. These potentials represent the lower energetic boundary for the reaction since nC_2 can have any amount of kinetic energy. The blue dashed line represents the potential for the initial state $C_{60} + X^+$. Landau–Zener theory assumes that the transfer between states only occurs in the region where these two potentials cross. The red dashed and dotted line represents internal bound states for $C_{60}^+ + X$. The energy of these bound states changes for different values of the angular momentum l (corresponding to different impact parameters). When the collision energy is roughly equal to that of one of these bound states, the chance of tunneling increases, causing a resonance.

Published under an exclusive license by AIP Publishing

The interior potential well was fit to a harmonic oscillator for several values of b and the top 20 states were calculated each time.[47,48] A list of states and their energies were obtained for all values of b that still allowed for an interior well. When a particle collides with roughly the same energy as one of these states, a resonance occurs. Each resonance was broadened using a Gaussian function and all the states were summed together to obtain the multiple resonance shape function $\sigma^*(\varepsilon)$, shown below,

$$\sigma^*(\varepsilon) = \sum_i \frac{1}{c\sqrt{2\pi}} \exp\left[-\frac{1}{2}\left(\frac{\varepsilon_i^* - \varepsilon}{c}\right)^2\right], \tag{10}$$

where c is the standard deviation of the Gaussian (which corresponds to the effective width of each state), the sum is over all the bound state energies (represented by ε_i^*) calculated previously. The shape function $\sigma^*(\varepsilon)$ is normalized to the total number of bound states ε_i^*. Broadening the energies using a Gaussian function has been used to take into account a variety of physical effects, such as deformation and vibrational excitation of the C_{60} carbon shell, Doppler broadening, lifetime broadening, and other possible broadening processes. The standard deviation c is the same for all states and is fit to the data from Christian *et al.* The entire function is scaled so the peak of the model is the same height as the peak of the data. This last step must be done since Christian only measured the relative cross sections.

The cross section for C_{60} charge transfer collisions with slow ions can be predicted by the Landau–Zener cross section[7,8,11] modulated by the resonance shape function $\sigma^*(\varepsilon)$. For illustration, the theoretical cross section for C_{58}^+ production from C_{60} colliding with oxygen cations is shown in Fig. 7 alongside the data digitized from Christian's paper.[23] In this example, the width of the Gaussian c was found to be 7.39 eVs.

Notice the peak of our potential shown in Fig. 4 has roughly the same energy as the peak of the fragmentation of a single C_2. Due to the size of C_{60}, a wide range of impact parameters will only shift the barrier up slightly. Most of the states calculated using our method have an energy slightly higher than this peak, causing a high density of states at the energy of the peak. Since each state corresponds to a resonance, a high density of energy levels creates a large peak in the cross section. Therefore, a peak in the potential barrier translates to a peak in the cross section. The curve overpredicts the cross section for a specific fragmentation for higher energies. This is consistent with Christian's explanation that the probability of one interaction is reduced through the opening of new reaction pathways, causing a reduction in the cross section. To account for this, we subtracted one cross section from the next and refit our cross sections for the final figures.

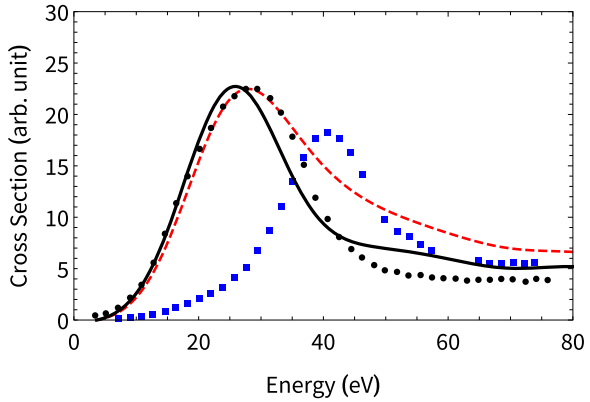

FIG. 7. Our model for $C_{60} + O^+$ cross sections shown alongside the measured cross sections.[23] The black dots represent data for an oxygen ion colliding with C_{60} and knocking off one C_2 leaving C_{58}^+. The blue squares represent data for an oxygen ion colliding with C_{60} and knocking off two C_2 leaving C_{56}^+. The red dashed line represents the cross section before accounting for a decrease in probability due to the opening of the $C_{56}^+ + 2C_2$ reaction channel. The black line represents our model after accounting for this reduction in cross section.

B. Landau–Zener model of interaction between different collisional channels

Landau–Zener model of nonadiabatic transitions between different states of compound systems assumes that the transfer between states is only possible when the energy of the two states is roughly the same.[10–12] This model was chosen because of its effectiveness and simplicity. When the two potentials get close to each other, the interaction between different diabatic states creates an avoided crossing. It is only at these avoided crossings that the diabatic state can change. Every time the projectile reaches the distance of a given crossing, there is some probability of transitioning between states. Given N number of states, each with only one crossing with the original state (Fig. 6 shows this scenario with $N = 4$), the probability of finishing in a particular state is

$$P_n = p_n \prod_{i=1}^{n} (1-p_i)\left[1 + \left(\sum_{j=n+1}^{N} p_j^2 \prod_{k=n+1}^{j-1} (1-p_k)^2\right) + \prod_{m=n+1}^{N} (1-p_m)^2\right], \tag{11}$$

where P_n is the probability of finishing in state n and p_n is the probability of remaining in the initial diabatic states at the crossing n. The probability to remain in the initial diabatic state at each one of the individual crossing points has been shown to be[10–12]

$$p = e^{-2v_x/v_l}, \tag{12}$$

where v_x is the characteristic velocity and v_l is the velocity at the turning point. The characteristic velocity is defined as

$$v_x = \frac{\pi V_{12}^2}{|V_{11}'(R_x) - V_{22}'(R_x)|}, \tag{13}$$

where $V_{11}'(R_x)$ and $V_{22}'(R_x)$ are the derivatives of the two potentials at the location of the crossing (R_x being the position of the crossing point). V_{12} is the interaction term of the Hamiltonian. V_{12} is difficult to calculate and is used as a fit parameter.

When the electron has been captured by the cation, it does not necessarily occupy any particular electronic state. Therefore, we calculate crossing points for multiple excited states. This leads to a system with many adiabatic regions predicted by the crossing points of the two potentials. The position of the regions of adiabatic transitions has been predicted using the potentials calculated previously,

Published under an exclusive license by AIP Publishing

shown in Figs. 4 and 5. To simplify the calculations required for our model, the potentials in Fig. 5 are used multiple times and are shifted down so that the energy at infinite distance is equal to the excited state energy. These shifted potentials represent different electronic excited states. The excited state energies for oxygen, nitrogen, and neon are all taken from Moore.[49]

Some of the crossings are located within the spherical shell. In order to access these inner crossings, the ion would have to penetrate C_{60} without destroying it. The C_{60} structure is not maintained during the interaction (since at least one C_2 is removed) and so the inner crossings were ignored. We also found that only two states are sufficient to get a reasonable fit, indicating that the resulting neutral atom is most likely in one of two states. Landau–Zener charge transfer theory predicts that the first crossing dominates the reaction and the impact of each subsequent crossing gets lower and lower. Therefore, the excited state with the lowest energy that still has more energy than the photoassociation energy of C_{60} (7.58 eVs) is overwhelmingly the most likely state the electron transfers into. For two crossings, Eq. (11) reduces to

$$P_1 = p_1(1-p_1)(1+p_2^2+(1-p_2)^2), \tag{14}$$

$$P_2 = 2p_2(1-p_2)(1-p_1). \tag{15}$$

Because the data do not differentiate between different electronic states of the resulting outgoing neutral atom, the total charge transfer cross section is the cross section of the two states added together. The interaction term of the Hamiltonian (V_{12}) of the two crossings and an overall magnitude parameter are all fit to the data. Since we are assuming that charge transfer and fragmentation are separate interactions, all the reactions start with pure charge transfer. Therefore, the total cross section for just charge transfer ($C_{60}^+ + X \rightarrow C_{60} + X^+$) is the sum of the cross sections for all the charge transfer and fragmentation reactions. The pure charge transfer cross section calculated for oxygen, nitrogen, and neon are all shown in Fig. 8.

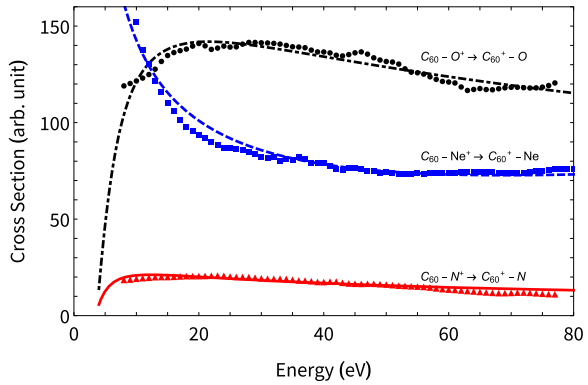

FIG. 8. The curves represent Landau–Zener charge transfer theory for two crossings where both interaction terms of the Hamiltonian were fit parameters. The crossing points were predicted from the potentials shown in Figs. 4 and 5. The points represent data taken by Christian *et al.*[21–23] The cross sections for all the different fragmentation reactions were summed together to produce the points shown.

Notice that the fundamental form of the neon charge transfer cross section is different from the other two ions. This decaying exponential like form fits well to crossing points with negative energy while the nitrogen and oxygen curves fit well to positive energy crossings. Our method predicts negative energy crossings only so they were shifted up by the photoionization energy of C_{60} to create positive energy crossings for nitrogen and oxygen.

VI. RESULTS

To obtain cross sections for C_{56}^+, C_{54}^+, and C_{52}^+ production, the potentials were shifted up in energy so that the peak in the potential energy had the same energy as the peak of the cross section of interest. The energy threshold for the detachment of C_2 molecules from fullerenes in collisions between C_{60} and different ions can depend on the type of heavy ion as well as the type of fullerene cation (C_{60}^+, C_{58}^+, C_{56}^+, C_{54}^+, or C_{52}^+). For the oxygen cation, we found the value of this shift to be about 10 eVs for all types of fullerenes, which is in line with the photo-fragmentation energy of C_{60}.[50–52] For C_{60} colliding with nitrogen and neon cations, shifts ranging from 4 to 8 eVs were found to produce more accurate results. Significant excitation of the rovibrational modes of fullerene cations by heavy ion projectiles can explain these differences from the photo-detachment data. The charge transfer cross sections shown in Fig. 8 are multiplied by the density of states shape function $[\sigma^*(\varepsilon)]$. As previously mentioned in Sec. V B, the opening of new channels takes away probability from previous channels. To account for this mechanism, the final step was to fit the data for C_{58}^+ to

$$\sigma_{C_{58}f} = a_1\ \sigma_{C_{58}} - b_1\ \sigma_{C_{56}}, \tag{16}$$

where $\sigma_{C_{58}}$ and $\sigma_{C_{56}}$ are the cross sections for the production of C_{58}^+ and C_{56}^+, respectively [obtained by multiplying the cross sections shown in Fig. 8 by the shape function $\sigma^*(\varepsilon)$]. Here, a_1 and b_1 are fit parameters and are related to the probabilities [P_n in Eq. (11)] of finishing in the single C_2 fragmentation or double C_2 fragmentation states. This was repeated for the other cross sections. The final results for oxygen, nitrogen, and neon are shown in Figs. 9–11, respectively.

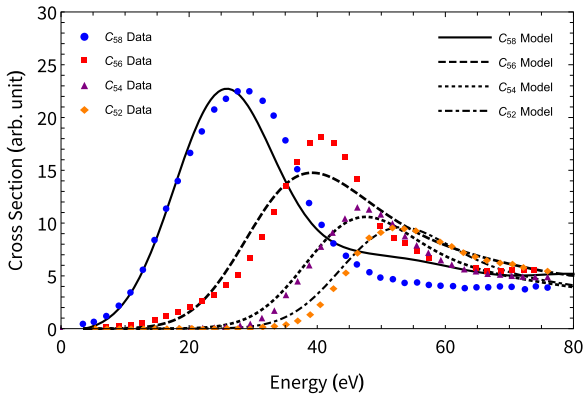

FIG. 9. The data from Christian *et al.*[23] for C_{60} colliding with O^+ plotted alongside our model (shown in black).

Published under an exclusive license by AIP Publishing

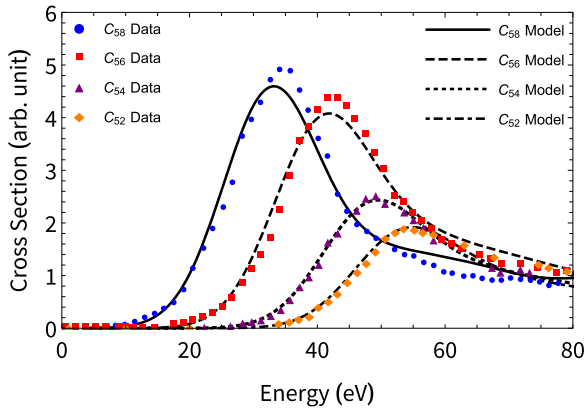

FIG. 10. The data from Christian *et al.*[22] for C_{60} colliding with N^+ plotted alongside our model (shown in black).

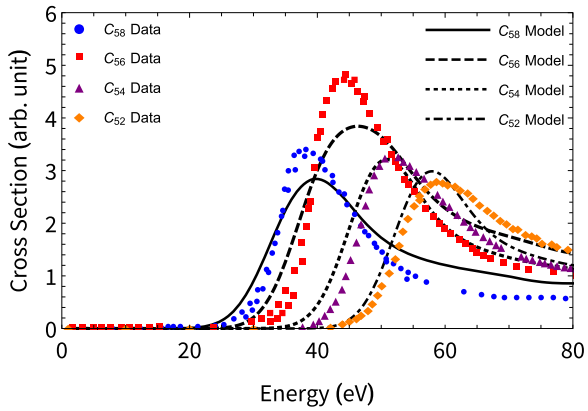

FIG. 11. The data from Christian *et al.*[21] for C_{60} colliding with Ne^+ plotted alongside our model (shown in black).

Our model is consistent with statements made by Christian *et al.*[23] Charge transfer occurs first leaving the $C_{60}^+ + X$ complex in an unstable excited state. This unstable state then decays, expelling some number of C_2 molecules. The cross section of all the fragmentation reactions is roughly constant and the cross section gets reduced with the opening of subsequent channels.

This model makes a few predictions about these fragmentation and charge transfer processes. Electrostatic forces create a high barrier at the radius of C_{60}, this barrier must be overcome for fragmentation to become likely. If the barrier is overcome with enough energy, more carbon atoms will be knocked loose. This barrier remains mostly unchanged for various impact parameters, which results in the resonances shown in our model. This implies the physical size of C_{60} plays a key role in these reactions. Landau–Zener charge transfer implies that the electron will most likely end up in the lowest excited state of the atom that still has more energy than the photoionization energy of C_{60}. Each subsequent energy level will have a smaller and smaller probability. Finally, the form of the pure charge transfer cross section is explained by Landau–Zener charge transfer theory. A positive energy crossing point creates a resonant like cross section, like the one shown for oxygen and nitrogen. A negative energy crossing point creates an exponential decay like cross section, like the one shown for neon.

ACKNOWLEDGMENTS

The work of M.B. and J.S. on this project was supported via UCLA Grant No. ONRBAA13-022. R.C. was supported by the National Science Foundation (NSF), Grant No. PHY-2034284. H.R.S. and V.K. acknowledge support from the NSF through a grant for ITAMP at the Center for Astrophysics | Harvard & Smithsonian. D.V. is also grateful for the support received from the National Science Foundation through Grant Nos. PHY-1831977 and HRD-1829184.

AUTHOR DECLARATIONS

Conflict of Interest

The authors have no conflicts to disclose.

Author Contributions

J. Smucker: Conceptualization (equal); Data curation (lead); Formal analysis (lead); Investigation (lead); Methodology (lead); Writing – original draft (lead); Writing – review & editing (equal). **J. A. Montgomery, Jr.:** Investigation (supporting); Visualization (supporting); Writing – review & editing (supporting). **M. Bredice:** Conceptualization (supporting); Methodology (supporting); Writing – review & editing (supporting). **M. G. Rozman:** Conceptualization (supporting); Investigation (supporting); Methodology (supporting). **R. Côté:** Conceptualization (supporting); Formal analysis (supporting); Funding acquisition (equal); Investigation (supporting); Supervision (supporting); Writing – review & editing (supporting). **H. R. Sadeghpour:** Conceptualization (supporting); Investigation (supporting); Methodology (supporting); Writing – review & editing (supporting). **D. Vrinceanu:** Conceptualization (supporting); Investigation (supporting); Methodology (supporting); Writing – review & editing (supporting). **V. Kharchenko:** Conceptualization (equal); Funding acquisition (equal); Investigation (supporting); Methodology (supporting); Supervision (lead); Writing – original draft (supporting); Writing – review & editing (equal).

DATA AVAILABILITY

Data sharing is not applicable to this article as no new data were created or analyzed in this study.

REFERENCES

[1] J. B. Delos, "Theory of electronic transitions in slow atomic collisions," Rev. Mod. Phys. **53**, 287 (1981).
[2] M. Tomza, K. Jachymski, R. Gerritsma, A. Negretti, T. Calarco, Z. Idziaszek, and P. S. Julienne, "Cold hybrid ion-atom systems," Rev. Mod. Phys. **91**, 035001 (2019).
[3] K. Dennerl, "Charge transfer reactions," Space Sci. Rev. **157**, 57–91 (2010).
[4] D. Rapp and W. E. Francis, "Charge exchange between gaseous ions and atoms," J. Chem. Phys. **37**, 2631–2645 (1962).

Published under an exclusive license by AIP Publishing

[5]D. Lyons, R. S. Cumbee, and P. C. Stancil, "Charge exchange of highly charged Ne and Mg ions with H and He," Astrophys. J. **232**, 27 (2017).
[6]M. S. Child, *Molecular Collision Theory* (Dover Publications, 1996).
[7]E. E. Nikitin and S. Y. Umanskii, *Theory of Slow Atomic Collisions* (Springer Science & Business Media, 2012), Vol. 30.
[8]N. F. Mott and H. S. W. Massey, *The Theory of Atomic Collisions* (Oxford University Press, 1965), Vol. 35.
[9]M. L. Goldberger and K. M. Watson, *Collision Theory* (Courier Corporation, 2004).
[10]R. E. Olson, J. R. Peterson, and J. Moseley, "Ion–ion recombination total cross sections—Atomic species," J. Chem. Phys. **53**, 3391–3397 (1970).
[11]R. E. Olson, "Two-state Stueckelberg-Landau-Zener theory applied to oscillatory inelastic total cross sections," Phys. Rev. A **2**, 121 (1970).
[12]C. Zener, "Non-adiabatic crossing of energy levels," Proc. R. Soc. London, Ser. A **137**, 696–702 (1932).
[13]J. Los and J. J. C. Geerlings, "Charge exchange in atom-surface collisions," Phys. Rep. **190**, 133–190 (1990).
[14]C. N. R. Rao and R. Voggu, "Charge-transfer with graphene and nanotubes," Mater. Today **13**, 34–40 (2010).
[15]P. A. Khomyakov, G. Giovannetti, P. C. Rusu, G. Brocks, J. Van den Brink, and P. J. Kelly, "First-principles study of the interaction and charge transfer between graphene and metals," Phys. Rev. B **79**, 195425 (2009).
[16]J. Jortner, M. Bixon, T. Langenbacher, and M. E. Michel-Beyerle, "Charge transfer and transport in DNA," Proc. Natl. Acad. Sci. U. S. A. **95**, 12759–12765 (1998).
[17]E. E. B. Campbell and F. Rohmund, "Fullerene reactions," Rep. Prog. Phys. **63**, 1061 (2000).
[18]G. Jnawali, Y. Rao, J. H. Beck, N. Petrone, I. Kymissis, J. Hone, and T. F. Heinz, "Observation of ground- and excited-state charge transfer at the C_{60}/graphene interface," ACS Nano **9**, 7175–7185 (2015).
[19]A. V. Akimov and O. V. Prezhdo, "Nonadiabatic dynamics of charge transfer and singlet fission at the pentacene/C_{60} interface," J. Am. Chem. Soc. **136**, 1599–1608 (2014).
[20]A.-M. Dowgiallo, K. S. Mistry, J. C. Johnson, and J. L. Blackburn, "Ultrafast spectroscopic signature of charge transfer between single-walled carbon nanotubes and C_{60}," ACS Nano **8**, 8573–8581 (2014).
[21]J. F. Christian, Z. Wan, and S. L. Anderson, "$Ne^+ + C_{60}$ collisions: The dynamics of charge and energy transfer, fragmentation, and endohedral complex formation," J. Chem. Phys. **99**, 3468–3479 (1993).
[22]J. F. Christian, Z. Wan, and S. L. Anderson, "$N^+ + C_{60}$ reactive scattering: Substitution, charge transfer, and fragmentation," J. Phys. Chem. **96**, 10597–10600 (1992).
[23]J. F. Christian, Z. Wan, and S. L. Anderson, "$O^+ + C_{60}$. $C_{60}O^+$ production and decomposition, charge transfer, and formation of $C_{59}O^+$. Dopeyball or $[CO@C_{58}]^+$," Chem. Phys. Lett. **199**, 373–378 (1992).
[24]J. F. Christian, Z. Wan, and S. L. Anderson, "C_{61}^+ production and decomposition in $^{13}C^+ + C_{60}$ collisions: C-atom exchange and the fragmentation pattern as a function of energy," J. Phys. Chem. **96**, 3574–3576 (1992).
[25]Z. Wan, J. F. Christian, and S. L. Anderson, "Collision of Li^+ and Na^+ with C_{60}: Insertion, fragmentation, and thermionic emission," Phys. Rev. Lett. **69**, 1352 (1992).
[26]A. D. Boese and G. E. Scuseria, "C_2 fragmentation energy of C_{60} revisited: Theory disagrees with most experiments," Chem. Phys. Lett. **294**, 233–236 (1998).
[27]C. Lifshitz, "C_2 binding energy in C_{60}," Int. J. Mass. Spectrom. **198**, 1–14 (2000).
[28]A. S. Baltenkov, S. T. Manson, and A. Z. Msezane, "Jellium model potentials for the C_{60} molecule and the photoionization of endohedral atoms, A@C_{60}," J. Phys. B **48**, 185103 (2015).
[29]A. Wüest and F. Merkt, "Potential energy curves of diatomic molecular ions from high-resolution photoelectron spectroscopy. I. The first six electronic states of Ar_2^+," J. Chem. Phys. **120**, 638–646 (2004).
[30]K. T. Tang and J. P. Toennies, "An improved simple model for the van der Waals potential based on universal damping functions for the dispersion coefficients," J. Chem. Phys. **80**, 3726–3741 (1984).
[31]K. Yabana and G. F. Bertsch, "Electronic structure of C_{60} in a spherical basis," Phys. Scr. **48**, 633 (1993).
[32]J. De Vries, H. Steger, B. Kamke, C. Menzel, B. Weisser, W. Kamke, and I. V. Hertel, "Single-photon ionization of C_{60^-} and C_{70^-} fullerene with synchrotron radiation: Determination of the ionization potential of C_{60}," Chem. Phys. Lett. **188**, 159–162 (1992).
[33]The full U_L values used for calculations are U_L = 0.881 786 019 6 a_0, U_L = 1.186 780 393 6 a_0 and U_L = 1.305 363 039 5 a_0 for d = 0.5 a_0, d = 0.32 a_0 and d = 0.28 a_0 respectively.
[34]T. Holstein, "Mobilities of positive ions in their parent gases," J. Phys. Chem. **56**, 832–836 (1952).
[35]F. Rohmund and E. E. B. Campbell, "Resonant and non-resonant charge transfer in C_{60}^++C_{60} and $C_{70}^+ + C_{60}$ collisions," J. Phys. B **30**, 5293 (1997).
[36]A. V. Glotov and E. E. B. Campbell, "Inelastic, quasi-elastic and charge transfer scattering in $C_{60}^+ + C_{60}$ collisions," Chem. Phys. Lett. **327**, 61–68 (2000).
[37]P. Schwerdtfeger, "The pseudopotential approximation in electronic structure theory," ChemPhysChem **12**, 3143–3155 (2011).
[38]V. Heine, "The pseudopotential concept," Solid State Phys. **24**, 1–36 (1970).
[39]I. V. Lindell, "Electrostatic image theory for the dielectric sphere," Radio Sci. **27**, 1–8, https://doi.org/10.1029/91rs02255 (1992).
[40]S. L. Ren, Y. Wang, A. M. Rao, E. McRae, J. M. Holden, T. Hager, K. Wang, W. T. Lee, H. F. Ni, J. Selegue, and P. C. Eklund, "Ellipsometric determination of the optical constants of C_{60} (buckminsterfullerene) films," Appl. Phys. Lett. **59**, 2678–2680 (1991).
[41]J. Ortiz-López and R. Gómez-Aguilar, "Dielectric permittivity and AC conductivity in polycrystalline and amorphous C_{60}," Rev. Mex. Fis. **49**, 529–536 (2003).
[42]A. Austin, G. A. Petersson, M. J. Frisch, F. J. Dobek, G. Scalmani, and K. Throssell, "A density functional with spherical atom dispersion terms," J. Chem. Theory Comput. **8**, 4989–5007 (2012).
[43]M. J. Frisch, G. W. Trucks, H. B. Schlegel, G. E. Scuseria, M. A. Robb, J. R. Cheeseman, G. Scalmani, V. Barone, G. A. Petersson, H. Nakatsuji, X. Li, M. Caricato, A. V. Marenich, J. Bloino, B. G. Janesko, R. Gomperts, B. Mennucci, H. P. Hratchian, J. V. Ortiz, A. F. Izmaylov, J. L. Sonnenberg, D. Williams-Young, F. Ding, F. Lipparini, F. Egidi, J. Goings, B. Peng, A. Petrone, T. Henderson, D. Ranasinghe, V. G. Zakrzewski, J. Gao, N. Rega, G. Zheng, W. Liang, M. Hada, M. Ehara, K. Toyota, R. Fukuda, J. Hasegawa, M. Ishida, T. Nakajima, Y. Honda, O. Kitao, H. Nakai, T. Vreven, K. Throssell, J. A. Montgomery, Jr., J. E. Peralta, F. Ogliaro, M. J. Bearpark, J. J. Heyd, E. N. Brothers, K. N. Kudin, V. N. Staroverov, T. A. Keith, R. Kobayashi, J. Normand, K. Raghavachari, A. P. Rendell, J. C. Burant, S. S. Iyengar, J. Tomasi, M. Cossi, J. M. Millam, M. Klene, C. Adamo, R. Cammi, J. W. Ochterski, R. L. Martin, K. Morokuma, O. Farkas, J. B. Foresman, and D. J. Fox, Gaussian~16 Revision A.03, Gaussian, Inc., Wallingford, CT, 2016.
[44]T. M. Miller and B. Bederson, "Atomic and molecular polarizabilities-A review of recent advances," Adv. At. Mol. Phys. **13**, 1–55 (1978).
[45]R. K. Nesbet, "Atomic polarizabilities for ground and excited states of C, N, and O," Phys. Rev. A **16**, 1 (1977).
[46]T. N. Olney, N. M. Cann, G. Cooper, and C. E. Brion, "Absolute scale determination for photoabsorption spectra and the calculation of molecular properties using dipole sum-rules," Chem. Phys. **223**, 59–98 (1997).
[47]J. N. L. Connor, "On the analytical description of resonance tunnelling reactions," Mol. Phys. **15**, 37–46 (1968).
[48]J. N. L. Connor, "On the semi-classical description of molecular orbiting collisions," Mol. Phys. **15**, 621–631 (1968).
[49]C. E. Moore, *Tables of Spectra of Hydrogen, Carbon, Nitrogen, and Oxygen Atoms and Ions* (CRC Press, 1993).
[50]K. Hansen, E. E. B. Campbell, and O. Echt, "The frequency factor in statistical fullerene decay," Int. J. Mass Spectrom. **252**, 79–95 (2006).
[51]B. Concina, S. Tomita, J. U. Andersen, and P. Hvelplund, "Delayed ionisation of C_{70}," Eur. Phys. J. D **34**, 191–194 (2005).
[52]B. Concina, K. Głuch, S. Matt-Leubner, O. Echt, P. Scheier, and T. D. Märk, "Metastable fractions and dissociations energies for fullerene ions C_n^+, 42 ≤ n ≤ 70," Chem. Phys. Lett. **407**, 464–470 (2005).

Published under an exclusive license by AIP Publishing